

SUPPLEMENTARY MATERIAL TO  
**Oxovanadium(IV) complexes of the pyridoxal Schiff bases:  
Synthesis, experimental and theoretical characterizations,  
QTAIM analysis and antioxidant activity**

PARISA GHORBANI<sup>1</sup>, S. ALI BEYRAMABADI<sup>2\*</sup>, MASOUD  
HOMAYOUNI-TABRIZI<sup>3\*\*</sup> and PARICHEHREH YAGHMAEI<sup>1</sup>

<sup>1</sup>Department of Biology, Science and Research Branch, Islamic Azad University, Tehran, Iran, <sup>2</sup>Department of Chemistry, Mashhad Branch, Islamic Azad University, Mashhad, Iran and <sup>3</sup>Department of Biology, Mashhad Branch, Islamic Azad University, Mashhad, Iran

*J. Serb. Chem. Soc.* 85 (1) (2020) 37–51

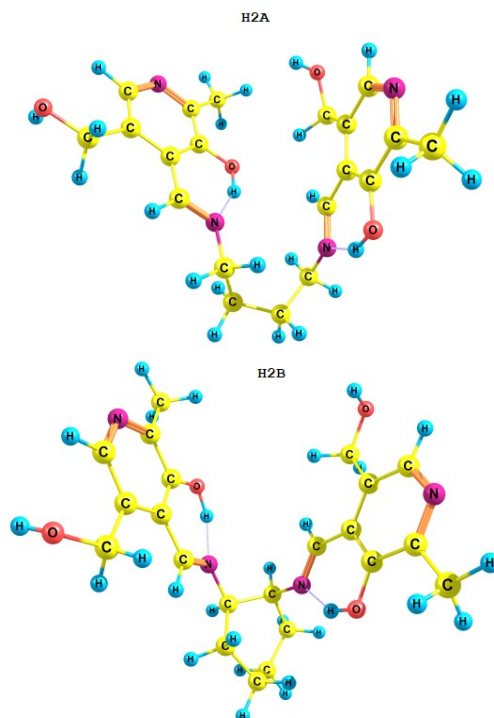


Fig. S-1. Optimized geometries of the H<sub>2</sub>A and H<sub>2</sub>B Schiff bases.

\*,\*\* Corresponding authors. E-mail: (\*)beiramabadi@yahoo.com,  
beiramabadi6285@mshdiau.ac.ir; (\*\*)mmhomayouni6@gmail.com

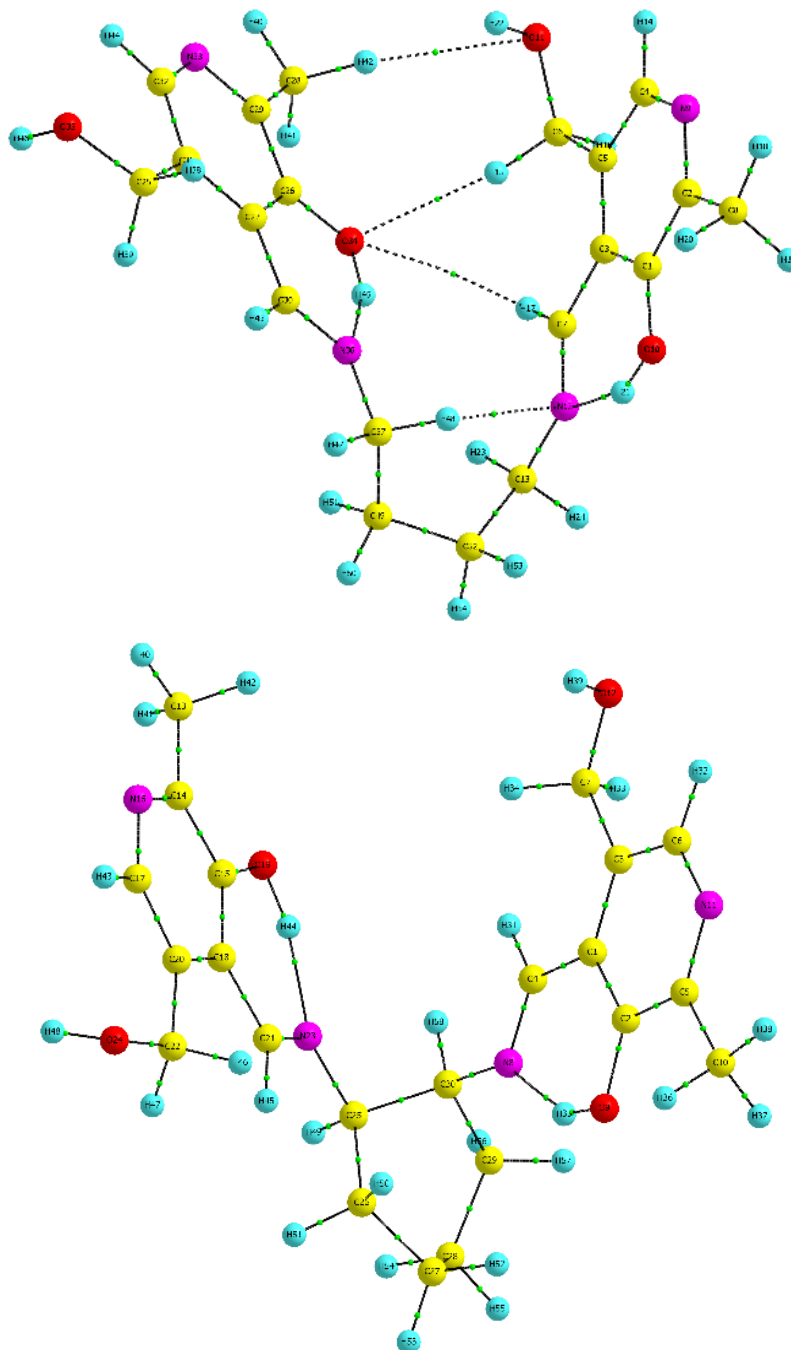


Fig. S-2. QTAIM molecular graph of the **H<sub>2</sub>A** and **H<sub>2</sub>B** Schiff bases. Small green spheres and lines correspond to the bond critical points (BCP) and the bond paths, respectively.

TABLE S-I. Selected experimental and theoretical IR vibrational frequencies ( $\text{cm}^{-1}$ ) and their computed intensity ( $\text{km mol}^{-1}$ ) for the [VO(A)] and [VO(B)] complexes

Exp.	[VO(A)]		Exp.	[VO(B)]		Vibrational assignment
	Theo.			Theo.		
	Frequency	IR Intensity		Frequency	IR Intensity	
542 (w)	511	39	556 (w)	539	61	$\nu_{\text{asym}}(\text{N2-V-N4})$
646 (w)	601	88	616 (m)	621	7	$\nu_{\text{asym}}(\text{O1-V-O2})$
	619	18		637	11	$\nu_{\text{sym}}(\text{O1-V-O2}) + \nu_{\text{sym}}(\text{N2-V-N4})$
745 (w)	727	51	759 (w)	739	39	Breathing of the pyridine ring
974 (m)	979	88	970 (m)	977	92	$\nu_{\text{sym}}(\text{C5-C16-O4, C11-C13-O3})$
	1006	19		1005	35	$\nu(\text{C17-N2, C19-N4})$
1023 (m)	1013	106	1058 (vs)	1021	170	$\nu(\text{V-O5})$
	1031	108		1033	118	$\nu(\text{C16-O4, C13-O3})$
	1075	27		1072	42	$\nu_{\text{asym}}(\text{C5-C16-O4, C11-C13-O3})$
	–	–		1063	23	$\nu(\text{C-C})$ cyclohexane ring
1189 (m)	1176, 1152	128, 142	1133 (s, sh)	1175	183	$\nu(\text{C=C, C=N})$ of the pyridine ring
1265 (m)	1242	57		1240	64	$\delta_{\text{ip}}(\text{H1, H4})$ pyridine ring
	1294	172		1300	180	$\nu(\text{py-C})$
	1329	28	1324 (m)	1323	42	$\delta_{\text{wag}}(\text{CH}_2)$ cyclohexane ring
1390 (vs)	1353	49		1353	67	$\delta(\text{CH}_3)$ Methyl
	1400, 1383	118, 323	1386 (s)	1400, 1388, 1378	103, 149, 246	$\nu(\text{C1-O1, C7-O2})$
	–	–		1438	11	$\delta_{\text{sci}}(\text{CH}_2)$ cyclohexane ring
	1449	93		–	–	$\delta_{\text{sci}}(\text{CH}_2)$ butane bridge
	1512 (s)	1551–1489	10–86	1545 (m)	1552–1490	19–108
1609 (s)	1578	500	1633 (s)	1586	585	$\nu(\text{C10-N4})$
	1595	260		1601	250	$\nu(\text{C6-N2})$
2856 (m)	2847	49	2851 (m, br)	2844	58	$\nu_{\text{sym}}(\text{CH}_2)$ of $-\text{CH}_2\text{OH}$
	2868	34		2867	35	$\nu_{\text{asym}}(\text{CH}_2)$ of $-\text{CH}_2\text{OH}$
	–	–		2906–2894	38–18	$\nu_{\text{sym}}(\text{CH}_2)$ cyclohexane ring
2925 (s)	2893	13		–	–	$\nu_{\text{sym}}(\text{CH}_2)$ butane bridge
	2917	14		2914	19	$\nu_{\text{sym}}(\text{CH})$ methyl
	–	–	2938 (vs, br)	2953–2946	42–54	$\nu_{\text{asym}}(\text{CH}_2)$ cyclohexane ring
	2958–2933	21–48		–	–	$\nu_{\text{asym}}(\text{CH}_2)$ butane bridge
3163 (s,br)	2966	–		3009	20	$\nu(\text{C6-H2, C10-H3})$
	3014, 2961	15, 14		3015, 2961	15, 18	$\nu_{\text{asym}}(\text{CH})$ methyl
3468 (s)	3089	2	3416 (s)	3090	2	$\nu(\text{C4-H1, C12-H4})$ aromatic
	3708	64		3709	60	$\nu(\text{O-H})$ of $-\text{CH}_2\text{OH}$

Abbreviation: wag, wagging; sci, scissoring; sym, symmetric; asym, asymmetric; ip, in-plane; w, weak; m, medium; s, strong; vs, very strong; sh, shoulder; br, broad.

TABLE S-II. The DPPH and ABTS radical scavenging activities (%) of the [VO(A)] and [VO(B)] complexes together with the BHA.

Concentration ( $\mu\text{g/mL}$ )	62.5	125	250	500
<b>DPPH radical</b>				
BHA	76.0	81.4	85.9	95.3
[VO(A)]	76.0	82.2	87.7	93.8
[VO(B)]	81.9	88.1	95.7	97.5
<b>ABTS radical</b>				
BHA	81.7	96.1	93.2	96.1
[VO(A)]	85.0	87.2	94.3	97.0
[VO(B)]	87.9	92.1	95.5	97.8